The 2004 North Slope of Alaska Arctic Winter Radiometric Experiment

Ed R. Westwater, Marian Klein, and Vladimir Leuski
Cooperative Institute for Research in Environmental Sciences, University of Colorado/NOAA-Environmental Technology Laboratory, 325 Broadway, Boulder, CO 80305, USA

Al Gasiewski, Taneil Uttal, and Duane Hazen
NOAA-Environmental Technology Laboratory, 325 Broadway, Boulder, CO 80305, USA

Domenico Cimini
Remote Sensing Division, CETEMPS, Universita' dell'Aquila, via Vetoio 1, 67010 Coppito, L'Aquila, Italy

Vinia Mattioli
Dipartimento di Ingegneria Elettronica e dell'Informazione
Università di Perugia, via G. Duranti 93, 06125 Perugia, Italy

Bob L. Weber and Sally Dowlatshahi
Science Technology Corporation
325 Broadway, Boulder, CO 80305, USA

Joseph A. Shaw
Department of Electrical and Computer Engineering, Montana State University
610 Cobleigh Hall, Bozeman, MT 59717, USA

Jim Liljegren and B. M. Lesht
DOE/Argonne National Laboratory, Bldg 203, 9700 South Cass Avenue
Argonne, IL 60439, USA

B. D. Zak
DOE/Sandia National Laboratories
PO Box 5800, MS 0755, Albuquerque, NM 87123, USA

Introduction

The importance of accurate measurements of column amounts of water vapor and cloud liquid has been well documented (Clough et al., 1999). Although several technologies have been investigated to measure these column amounts, microwave radiometers (MWR) have been used operationally by the Department of Energy's Atmospheric Radiation Measurement (ARM) program for passive retrievals of these quantities, which we call precipitable water vapor (PWV) and integrated cloud liquid (ICL). The technology of PWV and ICL retrievals has advanced steadily since the basic 2-

channel MWR was first deployed at ARM observation sites (Liljegren 2000). Two important advances are the development and refinement of the tipcal calibration method (Liljegren 2000, Han and Westwater 2000), and improvement of forward-model radiative transfer algorithms (Rosenkranz 1998). However, the concern still remains that current instruments deployed by ARM may be inadequate to measure low amounts of PWV and ICL. In the case of water vapor, this is especially important because of the possibility of scaling and/or quality control of radiosondes by the water amount (Clough et al. 1999). Extremely dry conditions, with PWV less than 3 mm, commonly occur in Polar Regions during the winter months. Accurate measurements of the PWV during such dry conditions are needed to improve our understanding of the regional radiation energy budgets. Jones and Racette (1998) show that the strength associated with the 183 GHz water vapor absorption line makes radiometry in this frequency regime suitable for measuring such low amounts. To investigate the promise of 183 GHz radiometry for measuring low amounts of PWV, an experiment was conducted by the NASA Goddard Space Flight Center (NASA/GSFC) and the NOAA Environmental Technology Laboratory (NOAA/ETL) at the ARM North Slope of Alaska/Adjacent Arctic Ocean (NSA/AAO) site during March of 1999. The recent experiment (Arctic Winter Water Vapor Intensive Operating Period 2004-WVIOP'04) was an outgrowth of these earlier theoretical considerations and experimental experiences. It was also intended to supplement efforts by industry (F. Solheim, Private Communication) to develop sub-millimeter wavelength radiometers for ARM deployment. In addition to quantitative improvement of water vapor measurements at cold temperature, the data will allow the evaluation of the sensitivity of millimeter-wave window channels to arctic clouds.

The WVIOP'04 was conducted at the NSA/AAO field site near Barrow, Alaska, during March 9 to April 9 2004. The major goal was to demonstrate that millimeter wavelength radiometers can substantially improve water vapor observations during the Arctic winter. Secondary goals included

forward-model studies over a broad frequency range, demonstration of recently developed calibration techniques, the comparison of several types of in situ water vapor sensors, and the application of infrared imaging techniques. During this IOP, radiometers were deployed over a broad frequency range (22.235 to 380 GHz), including several channels near the strong water vapor absorption line at 183.31 GHz. These radiometers were supplemented by frequent radiosonde observations and other in situ observations, including several "Snow White" Chilled Mirror radiosondes. The radiometers deployed will also be useful in measuring clouds during these cold conditions. Radiometers that were deployed include the Ground-based Scanning Radiometer (GSR) of NOAA/ETL (several frequencies from 50 to 380 GHz), the MWR and the Radiometric Profiler of ARM (frequencies from 22.235 to 60 GHz), and an infrared imager operated by Montana State University. In addition, all of the ARM active cloud sensors (radar and lidars) were operating. Preliminary results from this experiment are presented.

Recommendations from the NSA/AA0 March 1999 Experiment

During the NSA/AAO experiment in 1999, NASA/GSFC and NOAA/ETL deployed a suite of radiometers covering 25 channels in the frequency range of 20 GHz up to 340 GHz including 8 channels around the 183 GHz water vapor absorption line. Redundant measurements were made near 183 GHz and 340 GHz by two instruments, the Millimeter-wave Imaging Radiometer (MIR) and the Circular Scanning Radiometer (CSR). Vaisala RS80 radiosondes were launched daily at the field site, known as the “Great White”, as well as at the nearby National Weather Service (NWS) site in Barrow, where radiosondes containing the VIZ humidity sensor were launched. Based on our measurements and subsequent analysis, we made the following conclusions and recommendations for a follow-on experiment, again at the ARM NSA/AAO field site (Westwater et al. 2001).

(a) The theoretical basis of using 183 GHz radiometers to improve MWR retrievals of PWV at low amounts is sound. A variety of simulations and theoretical considerations all suggest that about 4% accuracy can be obtained during clear conditions, for PWV less than about 2.0 mm (Racette et al. 2004). During clear conditions and for the entire month of March, 1999, the total range of observed brightness temperature (T_b) at 23.8 GHz was about 3 K; the total range of 183 ± 7 GHz was about 80 K; i. e., the predicted increase in response to PWV was verified.

(b) Retrieval of PWV using millimeter-wave radiometric measurements is complicated by uncertainties that we outline. Very few ground-based measurements have been made at 183 GHz and, perhaps, not surprisingly, forward-modelled T_bs differ when different absorption models are used. Our calculations showed that substantial (~10 - 15 K) differences existed between the various models at some of the sub-millimeter frequencies. (Racette et al. 2004). Our estimated radiometric calibration accuracy allowed us to resolve some, but not all, of the problems. The uncertainties in RAOB measurements of water vapor, coupled with MIR and CSR calibration uncertainties of perhaps 3 K, did not allow us to make a clear choice between contemporary (Liebe and Layton 1987; Liebe, 1989; Liebe et al. 1993, Rosenkranz 1998) absorption models. This is not a fundamental limitation of the 183 GHz region, but reflects the fact that a more comprehensive database of Tb and high quality radiosonde measurements is needed.

(c) Comparisons of NWS radiosondes launched at Barrow with those that ARM launched at the CART site showed agreement in PWV usually in the range of about 0.05 cm, although simultaneous radiosondes were not available. Because of the long database of NWS radiosondes, and because currently, only one radiosonde per day is launched at the NSA/AAO site, a more definitive radiosonde comparison is recommended.

(d) It was discovered during the experiment, that the initial calibration of the ARM MWR was spurious because of poor thermal control. However, as was shown by Han and Westwater (2000)

that much of this problem was overcome when instantaneous, rather than averaged, calibration factors were used.

(e) For window frequencies and channels beyond perhaps ± 5 GHz from the absorption line center, sub-millimeter wave radiometer calibration can benefit by the tipcal method. Unfortunately, for the MIR radiometer during the 1999 experiment, two-sided tipcals were not possible, and hence some residual uncertainties existed. Again, this is not a fundamental limitation, but is one that can be overcome by equipment design.

(f) We also operated a scanning 5-mm radiometer during the March 1999 experiment; results of Racette et al. (2004) indicate that excellent temperature profiles can be derived from a scanning 5-mm radiometer if a radiosonde temperature profile is used for an initial guess. The availability of such data can improve sub-millimeter wave measurement-based retrievals in two ways: the derived profiles can be used to determine real-time mean radiating temperatures for tipcals. Second, the derived profiles can be scaled by MWR PWV measurements to provide a high quality first guess for 183 GHz retrievals.

Instruments Deployed at the NSA 2004 Arctic Winter Radiometric Experiment

NOAA/ETL designed and constructed a multi-frequency scanning radiometer operating from 50 to 380 GHz. The radiometers are installed into a scanning drum or scanhead (see Figure 1). The Ground-based Scanning Radiometer (GSR) uses the sub-millimeter scanhead with 11-channels in the 50-56 GHz region, a dual-polarization measurement at 89 GHz, 7-channels around the 183.31 GHz water vapor absorption line, a dual-polarized channel at 340 GHz, and three channels near 380.2 GHz. It also has a 10.6 micrometer infrared radiometer within the same scanhead. All of the radiometers use lens antennas and view two external reference targets during the calibration cycle. In addition, each of the radiometers' design includes two internal reference points for more frequent

calibration. The GSR instrument is a modification of the CSR that operated at the NSA/AAO site in 1999 (Westwater et al. 2001). A substantial improvement in radiometer calibration for ground observation in the Arctic environment has been achieved. Based on our experience from the 1999 IOP, a new set of thermally stable calibration targets with high emission coefficients were also designed, constructed, and deployed. The primary use of the instrument is to measure temperature, water vapor, and clouds, at cold (-20 to -55 °C) and dry (PWV < 5 mm) conditions. A schematic of the GSR is shown below in Figure 1. The beam widths of the GSR channels are 1.8 ° and can be averaged to given beam-widths that are consistent with the ARM MWR (4.5 to 5.5 °).

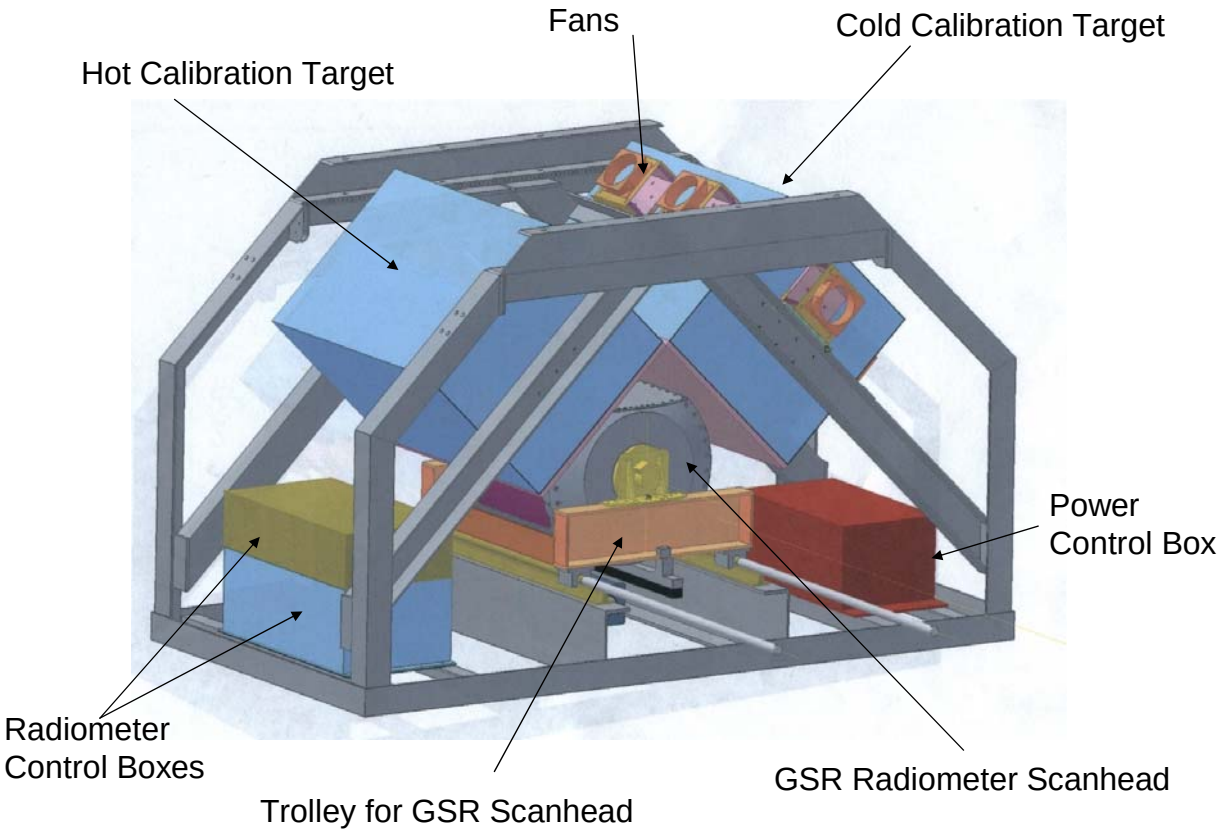

Figure 1. Schematic diagram of the GSR calibration and scanner system. The GSR scanhead periodically moves out of the framework for atmospheric viewing on a trolley system, and shares time observing the atmosphere and the two thermally controlled blackbody reference targets.

Figure 2. Photo of the GSR, the ARM Microwave Radiometer (MWR) and the ARM Microwave Profiler (MWPR) at the NSA/AAO Great White site near Barrow, Alaska.

In addition, the ARM MWR and the ARM Radiometric Profiler MWPR(Liljegren 2004) were also operated. The channels of the MWPR, in addition to providing temperature and humidity profiles, are also useful in forward model studies (Liljegren et al. 2004)..

The infrared cloud imager (ICI) is a ground-based infrared thermal imaging system used to identify and classify clouds based on the downwelling atmospheric radiance in the 8-14 um wavelength region. The ICI comprises an infrared camera using an uncooled micro-bolometer array, a gold-coated beam-steering mirror and a blackbody calibration source, controlled by software that can be accessed remotely (Shaw et al. 2003). The camera records images of the sky at a user-selected interval and relates the downwelling emission in each of 320 x 240 pixels to the state of cloudiness in that portion of the sky. Before each sky image, ICI performs an internal offset correction to minimize voltage variations across

the detector array, and then records an image of an extended-area blackbody source for radiometric calibration.

In addition, there were a variety of radiosonde data available. There were four-time-a day launches of ARM radiosondes that contain the Vaisala RS90 humidity element. Two of these launches coincided in time with the synoptic launches by the NWS in Barrow. Finally, we launched 10 "Snow White" Chilled Mirror radiosondes during clear conditions, on the same balloons as the ARM sondes. A summary of primary instruments that were deployed is shown in Table 1.

Table 1. Instruments deployed during the NSA/AAO Arctic Winter Radiometric Experiment

Platform	Parameters Derived	Frequencies (GHz)
ARM MWR	PWV, ICL	23.8, 31.4 GHz
GSR	PWV	183.31 ± 0.5, ± 1, ± 3, ± 5, ± 7, ± 12, ± 15 GHz
GSR	T, ICL	50.3, 51.76, 52.625, 53.29, 53.845, 54.4, 54.95, 55.52, 56.025, 56.215, 56.325 GHz
Microwave Profiler	T, PWV, ICL	22.235, 23.035 ,23.835, 26.235, 30.000, 51.250, 52.280, 53.850, 54.940, 56.660, 57.290, 58.800 GHz
GSR	ICL	89 GHz (dual-polarization)
GSR	PWV, ICL	340 GHz (dual-polarization)
GSR	PWV, ICL	380.2 ±4, ±9, ± 17 GHz
Infrared Cloud Imager	Spatial cloud coverage	8-14 microns
GSR	Cloud presence	10 microns
GPS	PWV	
Vaisala RS90 Radiosondes	T, P and ρ profiles	
Chilled Mirror Radiosondes	T, P and ρ profiles	
VIZ Radiosondes	T, P and ρ profiles	

Preliminary Data

Radiosondes

During the experiment a number of radiosondes were launched. The ARM Operational Balloon Borne Sounding System radiosondes (BBSS) were launched daily at 2300 UTC at the Great White. These systems used the Vaisala RS90 humidity elements. In addition, at the ARM Duplex, about 1 mile to the north from the Great White, BBSSs were launched four-times daily (500, 1100, 1700, and 2300 UTC). Raw data from synoptic radiosondes from the NWS (1100 and 2300 UTC) were also archived. Finally, during clear conditions, ten dual-sonde launches were conducted at the ARM Duplex. For these releases, five during the day and five during the night, the Chilled Mirror "Snow White" sondes were attached to the same balloon that carried the BBSS sensor. For the month of the experiment, a total of 220 soundings were taken. Figure 3 shows one result when four systems were launched at the same time. We think that the availability of the 220 radiosondes overcomes one of the principal limitations of the 1999 NSA/AAO experiment.

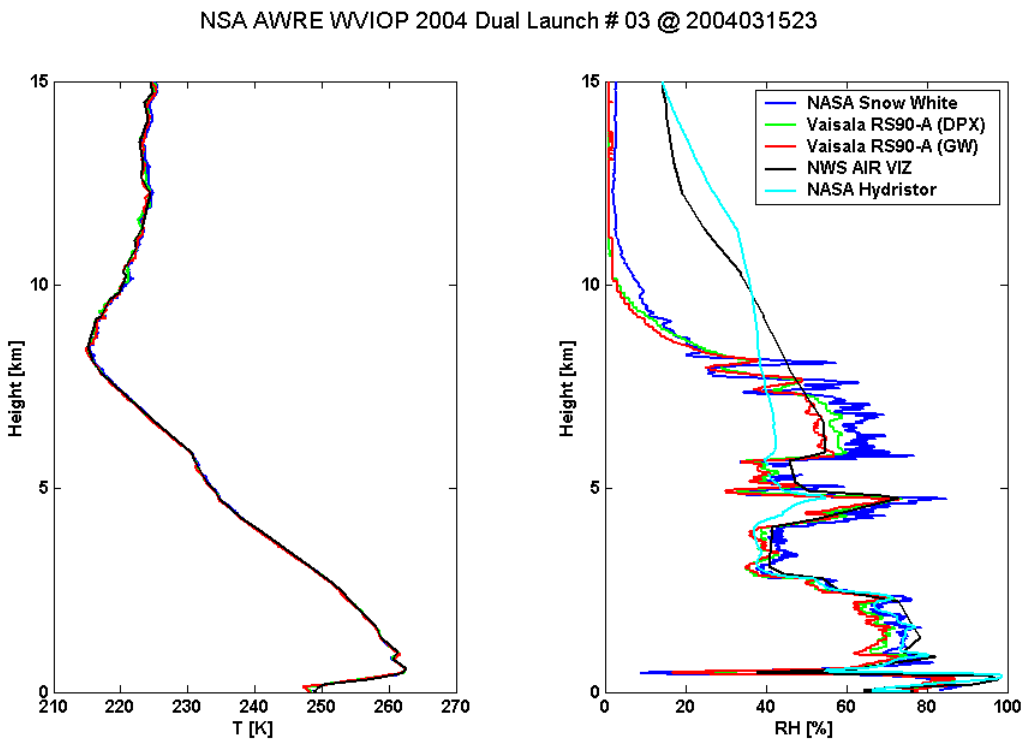

Figure 3. Comparisons of Radiosondes, including dual-sonde launch, on March 15 at 2300 UTC, Barrow, Alaska.

Comparisons of MWR, MWProfiler, and Tb's calculated from BBSS radiosondes

As discussed above, we launched Vaisala RS90 radiosondes from the ARM Duplex and from the Great White. As a preliminary evaluation of the quality of the data from the sondes, the MWR, and the MWProfiler, we compared the T_b data measured by the two radiometers with T_b calculated from the radiosondes, using the Rosenkranz 2003 absorption algorithm. The results, shown in Figure 4, are promising.

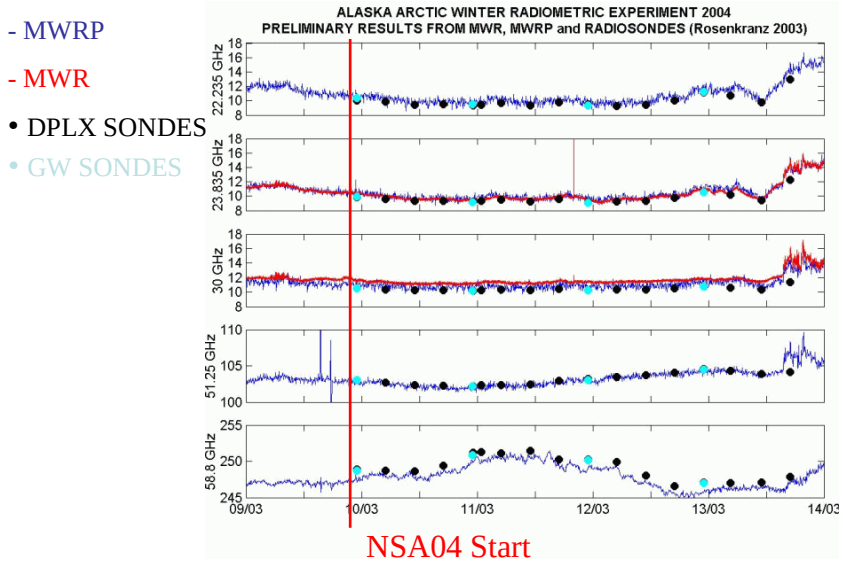

Figure 4. Comparison of T_b measured by ARM radiometers with calculations based on BBSS radiosondes and Rosenkranz 2003 absorption model.

Typical Target, continuous scan, and air-mass dwell for GSR.

The GSR has a flexible and software programmable angular-scanning sequence that is repeated every two minutes. The sequence starts with the GSR being inside the calibration house and viewing the hot calibration target for 3 seconds. During the next step, the GSR remains in the

calibration house and views the cold target, again for 3-seconds. The scanhead then moves out of the calibration house and moves to the atmospheric-scanning position, where it moves from air mass = 3.5 to a sequence of air mass dwells of 2-seconds each (air mass dwells at 3.5, 3.0, 2.5, 2.0, 1.5, 1.0, 1.5, 2.0, 2.5, 3.0, 3.5) . Between the air mass dwells the radiometer moves continuously to the next scan position. Thus the radiometer acquires both continuous and dwell data for the atmosphere with two-point calibration data in between. For channels in the transparency windows, both 2-point and tipcurve calibration methods can be used. In addition to the external calibration, the radiometer also switches between hot and cold internal calibration loads. Figure 5 shows the calibration sequence of the GSR.

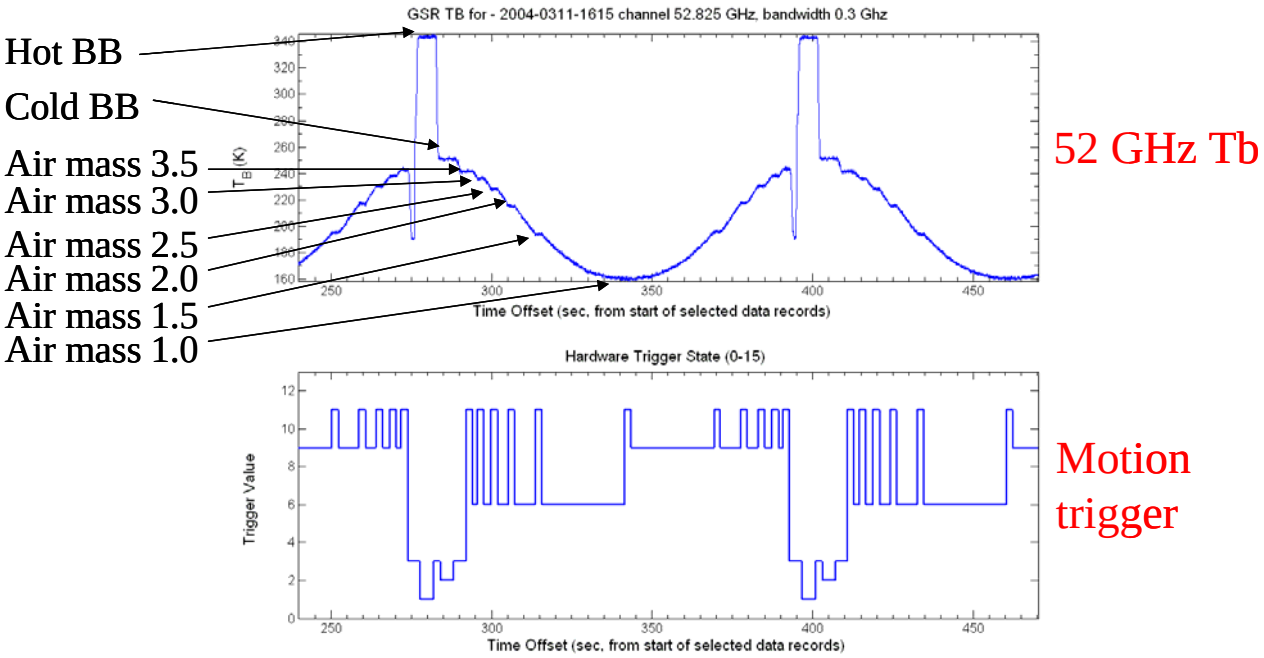

Figure 5. Calibration, dwell, and continuous scanning sequence of the GSR. Data taken on March 11, 2004, 1655 UTC.

Sample data from 50-60 GHz channels

As shown in Table 1, the GSR takes data at 11 channels in the 50-60 GHz Oxygen band. In Figure 6, we show a short series of data from these channels taken during the IOP. We note that

the strongest channels from 55.5 to 56.3 GHz clearly show the presence of a thermal inversion, i.e., T_b increases with increasing elevation angle... Conversely, the weakest channel at 50.3 GHz will allow tipcurve calibration. For all of the channels, the time spent dwelling at the separate air mass dwell points can be seen.

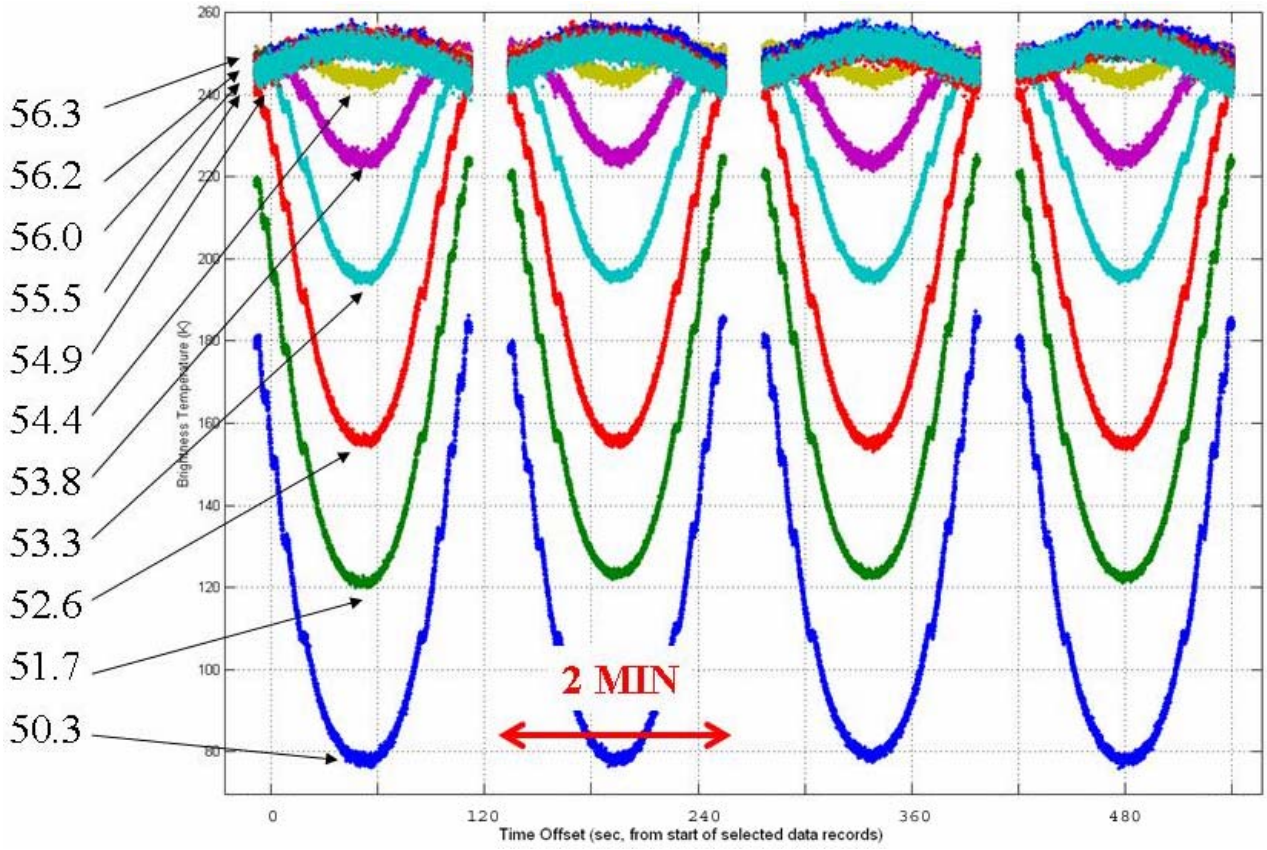

Figure 6. Time series of T_b between 50 and 60 GHz. See Figure 5 for date and time of data.

Sample data from 183.31 GHz channels

As shown in Table 1, the GSR takes data at 7 channels around the 183.31 GHz water vapor line. In Figure 7, we show a short series of data taken during the IOP. We note that the strongest channels from 183.31 ±0.5 and ±1 GHz are close to saturation; i.e., T_b is close to the kinetic temperature of the atmosphere. Conversely, the weakest channels from 183.31 ± 15, ±12, and

±7 GHz all will allow tipcurve calibration. Again. for all of these channels, the time spent dwelling at the separate air mass dwell points can be seen.

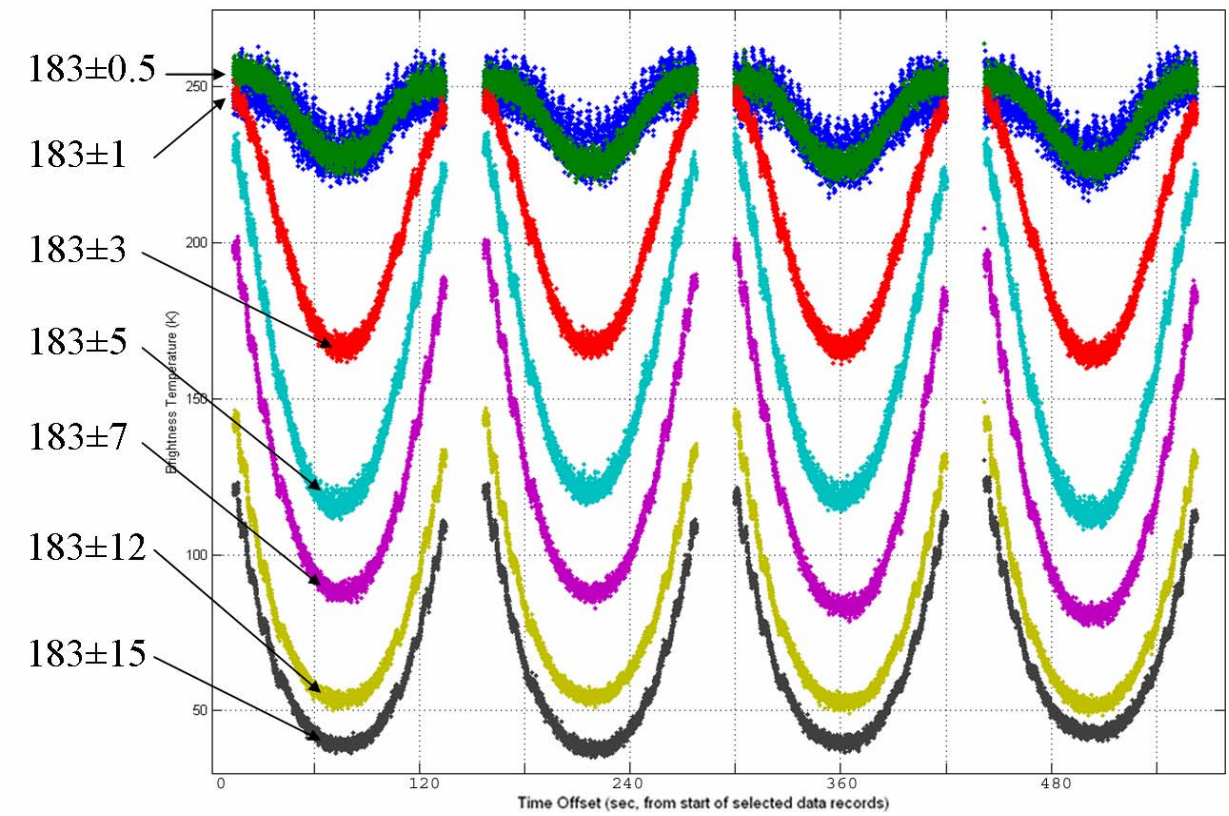

Figure 7. Time Series of T_b for channels around the 183.31 GHz water vapor line. See Figure 5 for date and time of data.

Sample data from 380.2 GHz channels

As shown in Table 1, the GSR takes data at 3 channels around the 380.2 GHz water vapor line. In Figure 8, we show a short series of data taken during the IOP. We note that the strongest channel at 380.2 ±4 GHz shows the presence of a thermal inversion.

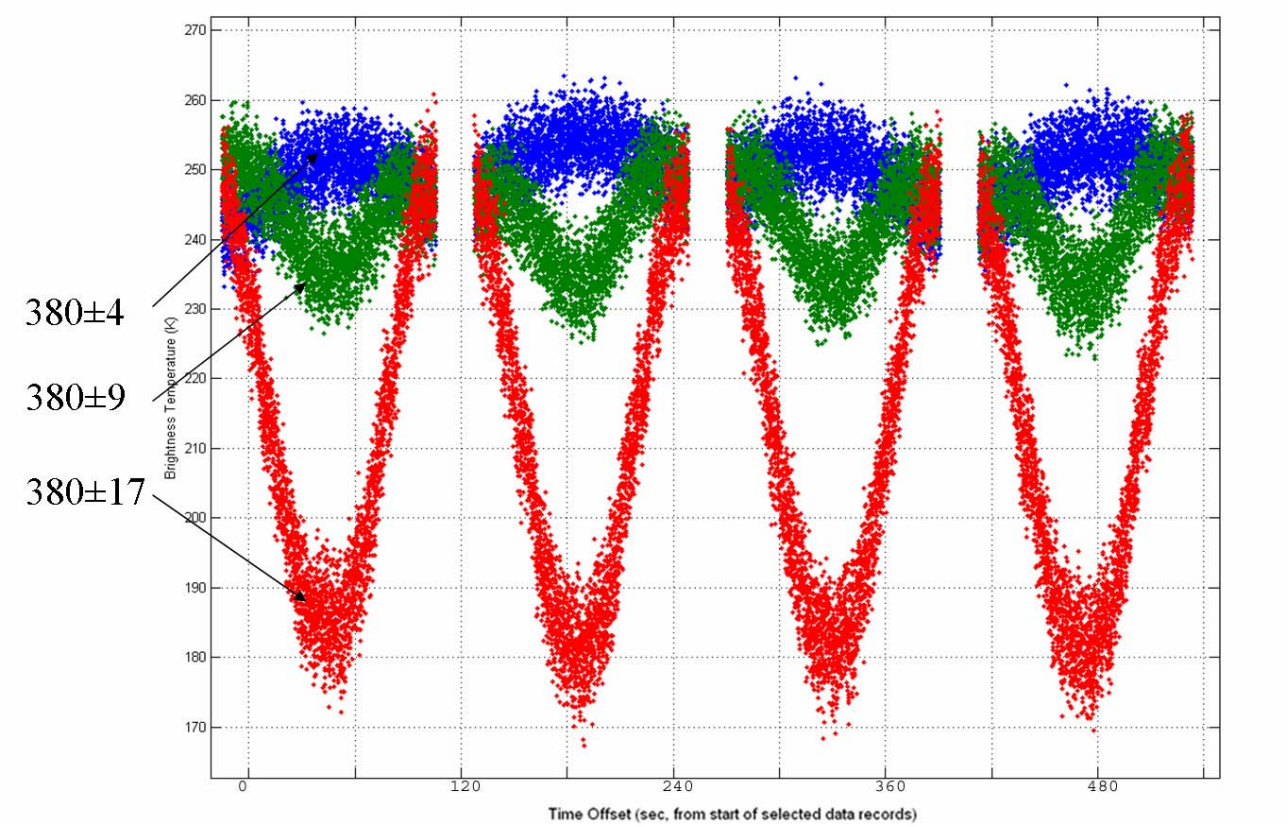

Figure 8. Time series of T_b near the 380.2 GHz water vapor line. See Figure 5 for date and time of data.

Data from the Infrared Cloud Imager

High quality images of the infrared radiance spectrum of the sky were obtained throughout the experiment by the ICI. A typical image is shown in Figure 9. We see the mixed cloud features with temperatures in the -20 ºC range, with the much colder clear sky portions of -50 to -60 ºC

.

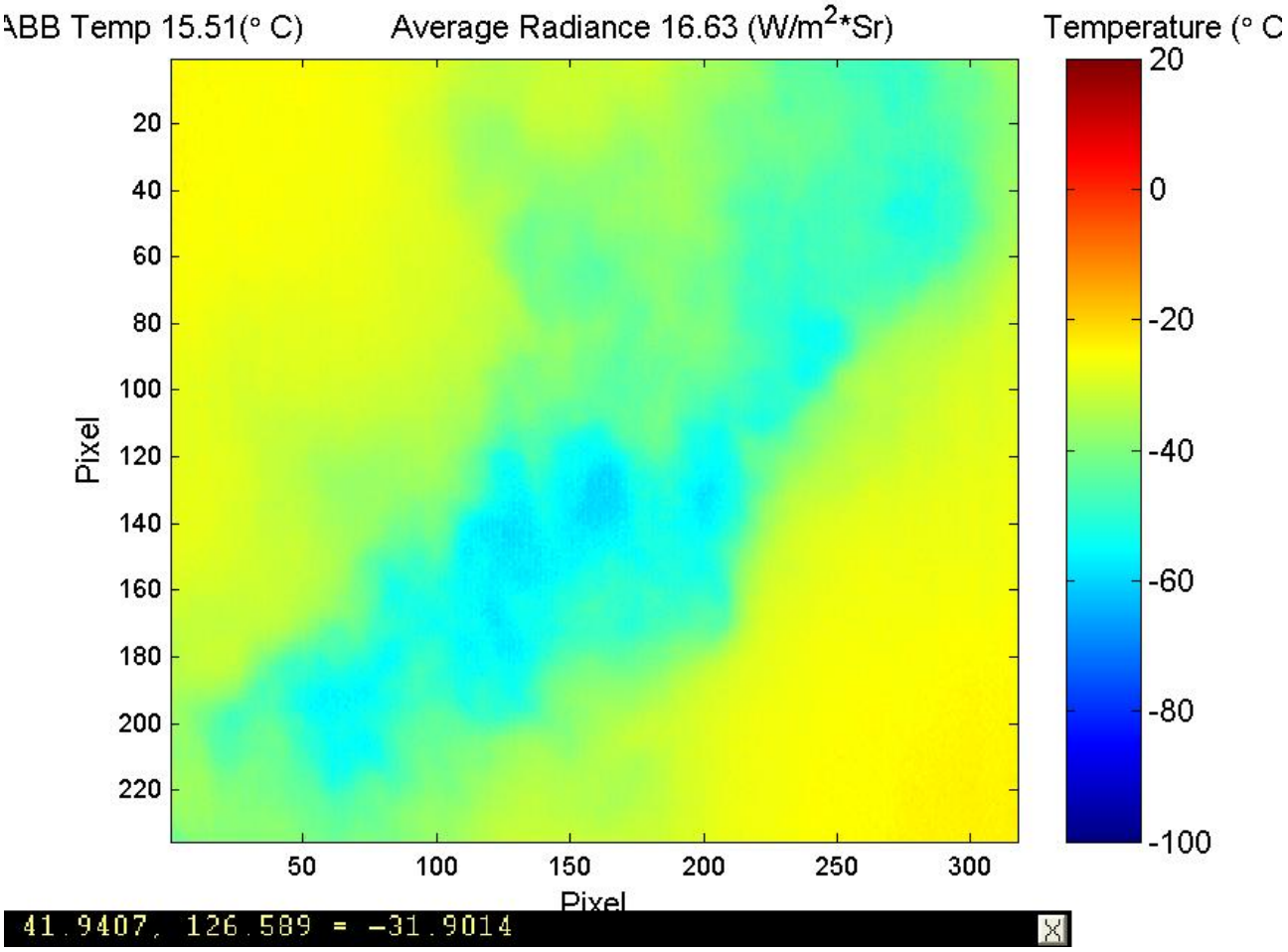

Figure 9. Infrared sky image obtained by the ICI during the NSA WVIOP'04.

Composite image of Cloud Radar, Micropulse Lidar, and MWR

Fortunately, even during the first few days of the IOP, a range of conditions was observed, ranging from a boundary-level liquid cloud, a mid-level ice cloud, completely clear, and mixed-phase clouds. An image of the first six days of the IOP is shown in Figure 10.

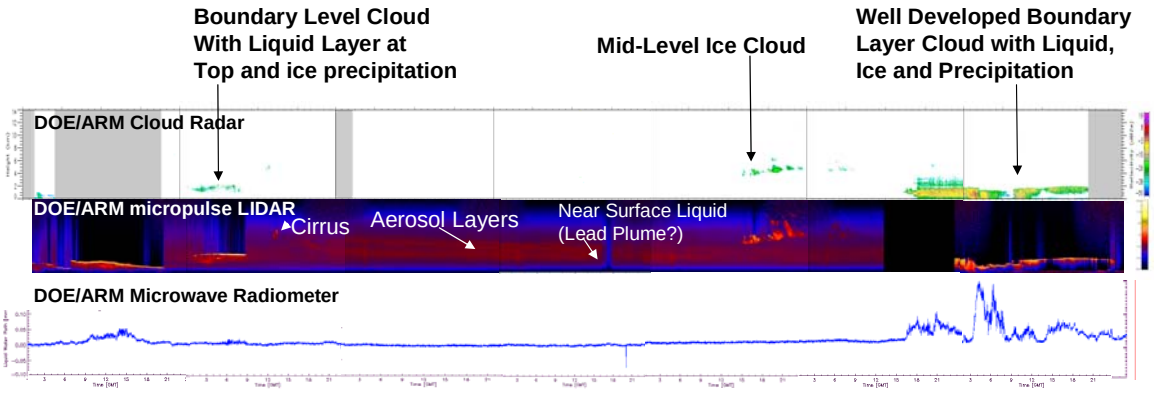

Figure 10. Composite image of cloud radar, Micropulse lidar and MWR observations for the first six days of the IOP. Clear sky, low cloud, mid-level clouds, mixed-phased clouds were observed.

Summary, Conclusions, and Further Work

The 2004 North Slope of Alaska Arctic Winter Radiometric Experiment was conducted from March 9 to April 9, 2004. It is already evident that an exceptionally rich data set of microwave and millimeter wavelength radiometric observations, infrared cloud images, and a comprehensive set of radiosonde observations were taken. Below is a short summary of the relevant observations.

(a) Radiosondes. A total of 220 radiosondes were launched during the 30-day period.

(b) The GSR operated flawlessly during the experiment.

(c) Both the MWR and MWRP operated and produced high quality data

(d) Both PWV from the MWR and temperature retrievals from the MWRP appear of high quality.

(e) The ICI operated continuously and yielded high resolution images of the sky every 2 minutes.

Further information on these data are available at: http://www.etl.noaa.gov/programs/2004/wviop/.

Our analysis plans using the data include:

(a) Data Screening and editing: Careful editing of data to remove outliers and radio frequency interference is the first priority.

(b) Investigate and compare calibration algorithms: Calibration opportunities include those using data from hot-cold targets, internal targets, and tip curves for the more transparent channels.

(c) Images of multi-channel data: For the GSR data, in which data were taken from a single platform and with a common time stamp, images of time series of these data can be produced. Images of the opacity of transparent channels may also be useful in determining clouds.

(d) Forward model studies during clear-skies: The models of Liebe87 (Liebe and Layton 1987; Liebe 1989), Liebe93 (Liebe et al. 1993), Rosenkranz98 (Rosenkranz 1998), Rosenkranz03 (P. W. Rosenkranz, Private communication), MONORTM (Delamere et al. 2002), and Liljegren et al. (2004) will be investigated. We will also derive best fit absorption parameters from the calibrated T_b and radiosonde data.

(e) Retrieval analysis: Because of the angular spectrum of multi-frequency radiometer data, the information content of several combinations of data can be analyzed. We will produce vertical profiles of temperature and humidity. Also, because of the multiplicity of radiosondes, many choices of several initial guess profiles are possible.

(f) Cloud studies: Using active remote sensing data from the cloud radar and lidar, we will conduct case studies when ice clouds and mixed phase clouds are present. First, using known cloud types, sensitivity studies of millimeter and microwave channels to clouds will be performed. These studies will be supplemented by radiative transfer modeling that includes scattering. We will also investigate cloud liquid profiling, using data from active and passive sensors.

Corresponding Author

Dr. Ed R. Westwater, Tel: 303-497-6527

Fax: 303-497-3577, email: Ed.R.Westwater@noaa.gov

URL: http://www.etl.noaa.gov/~ewestwater

Acknowledgements

The work presented in this paper was sponsored by the Environmental Sciences Division of the Department of Energy as a part of their Atmospheric Radiation Measurement Program.

References

Clough, S. A., P. D. Brown, D. D. Turner, T. R. Shippert, J. C. Liljegren, D. C. Tobin, H.E. Revercomb, and R.O. Knuteson, 1999: Effect on the Calculated Spectral Surface Radiances Due to MWR Scaling of Sonde Water Vapor Profiles, *Proc. of 9th Atmospheric Radiation Measurement (ARM) Science Team Meeting*.. [Available online at http://www.arm.gov/docs/documents/technical/conf_9903/index.html.]

Delamere J. S., S. A. Clough, E. J. Mlawer, S. Boukabara, K. Cady-Peirera, and M. Shepard, 2002: An update on Radiative Tranfer Model Development at Atmospheric and Environmental Research, Inc., Proc. of 12th ARM Science Team Meeting, 2002. [Available on line at http://www.arm.gov/publications/proceedings/conf12/extended_abs/delamere-js.pdf]

Jones, D. C. and P. Racette, (1998): Ground-based Retrieval of Very Low to High Columnar Integrated Water Vapor Using Combined Millimeter-wave and Microwave observations", *Proc. IGARSS'98*.

Liebe, H. J. 1989: MPM, an atmospheric millimeter wave propagation model, *Int. J. Infrared and Millimeter Waves*, **10**, 631-650.

Liebe, H. J. and D. H. Layton, 1987: Millimeter wave properties of the atmosphere: laboratory studies and propagation modelling, *NTIA Report 87-24*, 74 pp.

Liebe, H. J., G. A. Hufford, and M. G. Cotton, 1993: Propagation modeling of moist air and suspended water/ice particles at frequencies below 1000, in AGARD Conference Proceedings 542,

Atmospheric propagation effects through natural and man-made obscurants for visible through MM-wave radiation, pp. 3.1 to 3.10, Available from NASA Center for Aerospace Information, Linthicum Heights, MD, 1993.

Liljegren, J. 2000: Automatic self-calibration of ARM microwave radiometers, In *Microwave Radiometric Remote Sensing of the Earth's Surface*, P. Pampaloni and S. Paloscia (EDS), VSP2000, 443-441.

Liljegren, J. C. 2004: Improved retrievals of temperature and water vapor profiles with a twelve-channel radiometer, *Proc. 8th Symp. Integrated Observing and Assimilation Systems for Atmospheres, Oceans, and land surfaces* (IOAS-AOLS) Seattle, WA, Amer. Met. Soc., 11-15 January 2004.

Liljegren, J. C., S. A Boukabara, K. Cady-Pereira, S. A Clough, 2004: The Effect of the Half-Width of the 22-GHz Water Vapor Line on Retrievals of Temperature and Water Vapor Profiles with a Twelve-Channel Microwave Radiometer , Submitted to *IEEE Trans. Geosci. And Remote Sensing*

Han, Y. and E. R. Westwater, 2000: Analysis and improvement of tipping calibration for ground-based microwave radiometers, *IEEE Trans. Geosci. Remote Sensing*, **38**, 1260-1275, 2000.

Rosenkranz, P. W., Water vapor microwave continuum absorption: A comparison of measurements and models, *Radio Sci.*, **33**, pp. 919-928 (1998a). Correction, *Radio Sci.*, **34**, p. 1025 (1999).

Racette, P. E., E. R. Westwater, Y. Han, A.J. Gasiewski, M. Klein, D. Cimini, D. C. Jones, W. Manning, E. J. Kim, J. R. Wang, V. Leuski, P. Kiedron (2004):"Measurement of Low Amounts of Precipitable Water Vapor Using Ground-Based Millimeter-wave Radiometry", Submitted to *J. Atmos. Oceanic. Technol*.

Shaw, J. A., and B Thurairajah. 2003: Short-term cloud statistics at NSA from the infrared cloud imager. In *Proceedings of the Thirteenth Atmospheric Radiation Measurement (ARM) Science Team Meeting*, [Available online at http://www.arm.gov/docs/documents/technical/conf_0304/shaw-ja.pdf]

E. R. Westwater, E. R., Y. Han, V. G. Irisov, V. Leuskiy, E. N. Kadygrov, and S. A. Viazankin, , 1999: Remote Sensing of Boundary-Layer Temperature Profiles by a Scanning 5-mm Microwave Radiometer and RASS: Comparison Experiment, *J. Atmos. Oceanic Technol*., **16(7)**, 805-818.

Westwater, E. R., P. E. Racette , and D. Cimini, 2001: The Arctic Winter Millimeter-Wave Radiometric Experiment: Summary, Conclusions, and Recommendations, *Proc. of 11th Atmospheric Radiation Measurement (ARM) Science Team Meeting*, March 19-23, 2001 [Available online at http://www.arm.gov/docs/documents/technical/conf_0103/index.html.]